PROPERTIES OF EJECTA GENERATED AT HIGH-VELOCITY PERFORATION OF THIN BUMPERS MADE FROM DIFFERENT CONSTRUCTIONAL MATERIALS

N.N. Myagkov[(1)], T.A. Shumikhin[(1)], L.N. Bezrukov[(2)]

[(1)] Institute of Applied Mechanics of RAS, Leninsky prospect 32A, Moscow 119991, Russia Email: tish2002@mail.ru
[(2)] GosNIIAS, 7 Victorenko street, Moscow 125319, Russia Email: bezrukov@gosniias.ru

ABSTRACT

The series of impact experiments were performed to study the properties of ejecta generated at high-velocity perforation of thin bumpers. The bumpers were aluminum plates, fiber-glass plastic plates, and meshes weaved of steel wire. The projectiles were 6.35 mm diameter aluminum spheres. The impact velocities ranged from 1.95 to 3.52 km/s. In the experiments the ejecta particles were captured with low-density foam collectors or registered with the use of aluminum foils. The processing of the experimental results allowed us to estimate the total masses, spatial and size distributions, and perforating abilities of the ejecta produced from these different bumpers. As applied to the problem of reducing the near-Earth space pollution caused by the ejecta, the results obtained argue against the use of aluminum plates as first (outer) bumper in spacecraft shield protection.

1 INTRODUCTION

The perforation of a thin plate by a high-velocity projectile may lead to fragmentation of the projectile with the formation of a cloud of after-impact fragments expanding into the semi-space behind the perforated plate. The other possible consequence of such an event is the generation of ejecta particles which propagate into the other semi-space, the one from where the projectile came.

Due to the ejecta phenomenon, a high-velocity encounter of a meteoroid or a space debris particle with a spacecraft surface produces the ejecta particles, which may represent a danger to exterior equipments of the spacecraft (the antennae, solar batteries, etc) [1]. Nowadays, the ejecta particles are considered as one of the main sources of the near-Earth space pollution [1, 2] that justifies an interest to their study.

In this work, we present the series of impact experiments, which were performed to study the properties of ejecta generated at high-velocity perforation of thin bumpers made from different constructional materials. Moreover, a comparative evaluation of the ejecta generated in the experiments may help us to form recommendations for reducing the near-Earth space pollution with the ejecta by means of the bumper material selection. In the experiments the bumpers were the aluminum plates, the fiber-glass plastic plates and the meshes weaved of steel wire. The projectiles were substantially the 6.35 mm diameter aluminum spheres and 3.2 mm spheres in several experiments. In the experiments the ejecta particles were captured with low-density foam collectors or registered with the use of aluminum foils.

The choice of the bumpers was dictated by the following considerations. The thin aluminum plate is the classic bumper providing protection against a meteoroid or a space debris particle for manned spaceship. The mesh bumpers are also used in spacecraft protective shields (see, for example, "Mesh Double-Bumper" [3] and protection of the Russian ISS module "Zarya" [4]). Non - metallic composite materials, especially fiber-glass plastics, are widely used in space technologies because of their high strength ability combined with relatively low density.

2 SETUP OF THE EXPERIMENTS

The general scheme of the experiments is presented in Fig. 1. A two-stage light-gas gun accelerates the sabot with a projectile up to velocities ~ 3.5 km/s. In the expansion chamber the couple of steel annular cutoffs separates the projectile from the sabot and the projectile moves further into the target chamber where the velocity-meter registers its velocity. The target is fixed in the end part of the target chamber. The interaction of the projectile with the target generates ejecta particles which penetrate into the collector placed in front of the target.

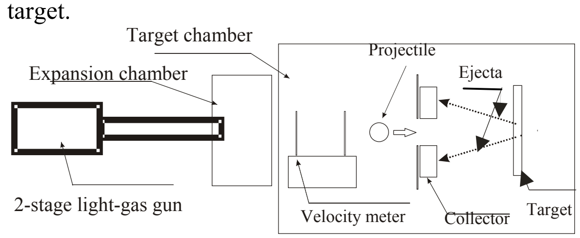

Fig. 1 The scheme of experiments with collectors

2.1 Experiments with low-density collectors

A scheme of experiments with low-density foam collectors shown in Fig. 2 was used for experiments with metallic bumpers. The collectors were made of 15 kg/m^3 polystyrene foam. They had a cylindrical form

Proc. '6th European Conference on Space Debris'
Darmstadt, Germany, 22–25 April 2013 (ESA SP-723, August 2013)

and consisted of two parts (Fig. 2). The main part had height of 100 mm and diameter of 250 mm. The other collector part was a ring with height of 50 mm and internal diameter of 130 mm. The shell of the collector consisted of the metallic cylinder with the frontal part closed by the metallic lid with an entrance hole for the projectile. The lid was screened by the wood protective shield to prevent possible damages by the shot debris. The target was clasped to the collector ring by a special frame so that the plane of the target coincided with the back side of the ring (Fig. 3). The collector camera was the room which was completely enclosed by the target surface and the inner surfaces of the collector parts.

To extract the captured ejecta particles we used some available solvents. The extracted particles were weighted using the high-accuracy electronic laboratory balance. The recovered substance was also studied using a metallurgical microscope. The extracted particles provided information about their sizes, masses, spatial and size distributions, and after-impact phase states.

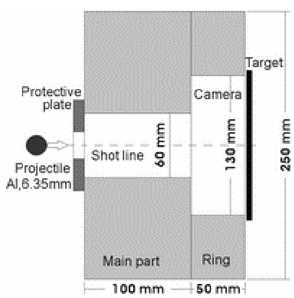

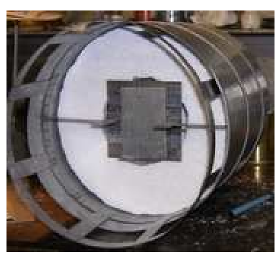

Fig. 2. The cross-section of the collector along the shot line.
Fig.3. The view of the collector with the attached target before its installation in the target chamber.

In all experiments with the foam collectors (Table 1) we used 6.35 mm diameter projectiles of 2017 or AD1 aluminum alloy (the projectile mass was ~ 0.39 g). The bumpers were AMg6 aluminum plates of 1.45 mm and 3.0 mm thickness, and meshes weaved of steel wire with l_a x d_w = 2.0 mm x 1.0 mm and 1.0 mm x 0.32 mm where d_w is the wire diameter and l_a is the aperture (inside light visible distance between adjacent wires). All impacts were normal to the target surface.

2.2 Experiments with foils as collectors

From the very beginning it was obvious that in the case of the non-metallic composite targets the recovering of ejecta particles from polystyrene foam would be a quite difficult (rather impossible) problem. Therefore a different scheme of experiments was used. According to that scheme the sheets of aluminum foils were situated in front of a tested target (Fig. 4). This scheme was used in experiments with the fiber-glass plastic plates and the AMg6 aluminum plates as targets. The total number, spatial and size distribution, and perforating ability of ejecta particles can be assessed using such a simple scheme.

The fiber-glass plastic material KAST-V with density 1.87g/sm^3 and another one, VFT-R, possessing more thermo-resistance ability and having density 1.84 g/sm^3, were chosen for the experiments. They both are made from the layers of fiber-glass fabric with bonding agent made on the base of epoxy and phenol- formaldehyde resins. The volume of the fiber glass is about 70% in the composite.

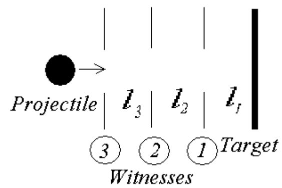

Fig. 4. The scheme of experiments with aluminum foils (#1, 2 and 3) as collectors. l_1, l_2 and l_3 mean distances.

In the experiments the 2 mm-thick fiber-glass plastic plates having ~3.7 kg/m^2-areal density were chosen as targets (in fact the usage of plates or other flat sheet-like structural elements with density high than 3-4 kg/m^2 is hardly possible in a spacecraft construction). Three experiments were carried out using AMg6 aluminum plates of 1.45 mm and 3.0 mm thickness as targets. In the experiments we used the 6.35 mm and 3.2 mm diameter projectiles of 2017 aluminum alloy. The projectile velocities ranged from 2.0 to 3.5 km/s; all impacts were normal to the target surface. The data for all experiments with foils as collectors are shown in Tab.5.

It is worth to note that some efforts were undertaken to find the most appropriate parameters in the experiment scheme, such as the distances between foils and the foil thicknesses, to get better ejecta fixation. As a result of the preliminary experiments, we came to the following setups: three 0.06 mm-thick aluminum foils for fiber-glass plastic targets and couple of 0.2 mm-thick aluminum foils together with third 0.06 mm-thick aluminum foil for aluminum plate targets; the distance between the target and the first foil was 50 mm or 100 mm, and that between the other foils was from 20 mm to 40 mm.

3 RESULTS OF THE EXPERIMENTS

3.1 Results of experiments with metallic bumpers and low-density collectors.

Thirteen experimental shots occurred to be appropriate for examination and analysis. They are presented in Tab. 1.

Fig. 5 and 6 present the face of the main parts of collectors C01 and C07 (Tab. 1) from the experiments with the aluminum plates. The inspection of the collectors shows that the matter in the ejecta is distributed quite inhomogeneously forming deep channels in the foam collectors (up to 100 mm in length and several millimeters in width in the experiments with the 3 mm-thick aluminum plate). The channels could be formed either by the single particles with the size of about 1 mm or by the jets consisting of the smaller ejecta particles. In fact, the imprints of the thread-like vertical traces of small holes (Fig. 7 and 8) on the side wall of the collector camera show that the matter in the ejecta is concentrated in the jets whose angles change during the process of the target perforation. The jets form an ejecta cone. It is worth to note that on the side walls of collectors C01 and C07 deep channels are not observed. Seemingly the angle of the ejecta cone measured from the shot line increases starting with the lower angle where intensity of the jets has a maximum value.

Fig. 5. Face side of the collector C01

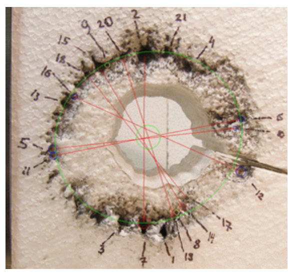

Fig. 6. Enumerated craters on the face side of collector C07

Fig. 7. Side wall of the collector C01 ring with vertical chains of holes

Fig. 8. Side wall of the collector C07 ring with vertical chains of holes.

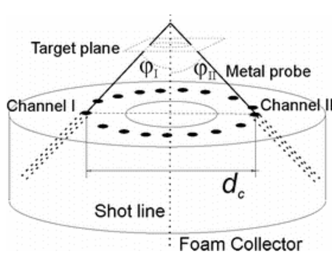

Fig. 9. Scheme of assessment of the ejecta trajectory angles using the probes

In Fig.5 (collector C01) the ejecta cone left the traces distributed along a circle whose diameter was bounded within the range of 108 to 119 mm. The perforation hole in the 1.45 mm-thick plate (shot C01) had the diameter about 8 mm. The calculation of the angles of the ejecta cone measured from the shot line gives the values from 45 to 48 degree. In case of the 3 mm-thick plate as target in shot C07 (Fig.6) the diameter of the circle of the cone traces is within the range of 94 to 104 mm that with the 13.2 mm diameter of the perforation hole gives the angles of the ejecta cone in the range of 39 to 42 degree. Shot C08 (the case of the 3 mm-thick plate too) reveals the angles of the ejecta cone in the range of 40 to 42 degrees.

As it was noted above, the impact on the 3 mm-thick aluminum plate generates quite intensive ejecta, which form channels in the collector with diameters up to several millimeters. The latter allowed us to estimate the ejecta angles more accurately. For this purpose a couple of thin metal probes were used as shown in Fig.9. In the figure φ_I and φ_{II} denote the angles (measured from the shot line) corresponding to channels I and II, and d_c is the distance between these channels. Fig. 6 presents the linked couples of opposite channels whose angles were estimated. The angles and channel-to-channel distances for shot C07 are presented in Tab. 2. Since the ejecta traces form rather an ellipse than a circle, the data for the angles should be divided into two groups corresponding to the major and minor diameters of the ellipse. The average angle for the major diameter is 42 degrees and for the minor one is 37 degrees. These data for the ejecta angles obtained by the direct measurements coincide approximately with the data presented above. Similar measurements of the cone angles were made for collector C01 (experiment with the 1.45 mm-thick aluminum plate). The comparison of the ejecta angles corresponding to the experiments with the 1.45 mm-thick plate and the 3.0 mm-thick one (Tab. 3) allows us to draw the conclusion that the angle of ejecta cone (measured from the shot line) depends on the thickness of the plate, so that the angle is lower for thicker plate. This conclusion agrees, for example, with result obtained in [5] (see Eq. (1) in [5] obtained on the basis of empirical data and numerical calculations).

The total masses of the ejecta particles recovered from the collectors are presented in Tab. 1. One can see that the total ejecta mass in the experiments with the meshes is sufficiently lower than that in the experiments with the plates. The total ejecta mass increases together with the plate thickness. The pictures of the ejecta particles recovered from collectors C11, C03 and C18 are presented in Fig. 10, 11 and 12. Actually, even the visual examination of the recovered substance shows the significant difference between the solid and mesh targets of equal areal density in Fig. 10 and 11. The characteristic peculiarity of the ejecta from the 3 mm-thick aluminum plate (Fig. 12) is that the bigger part of the recovered mass consists of quite large particles.

Masses and sizes of the ejecta particles recovered in the experiments (shots C11, C03 and C18) are presented in Tab. 4, where the particle sizes are specified for the two largest dimensions *L* and *W*. One can see that in the experiments with the aluminum plates the size of the ejecta particles reaches ~4 mm that exceeds the projectile radius. Tab. 4 also shows the significant difference between the sizes of the ejecta particles obtained in the experiments with the solid and mesh targets of equal areal density. Fig. 10-12 and Tab. 4 show comparative assessment, which is typical also for other shots from Tab. 1.

Fig. 10. Recovered ejecta particles from collector C11 (steell mesh).

Fig. 11. Recovered ejecta particles from collector C03 (1.45 mm-thick plate)

Fig. 12. Recovered ejecta particles from collector C18 (3.0 mm-thick plate).

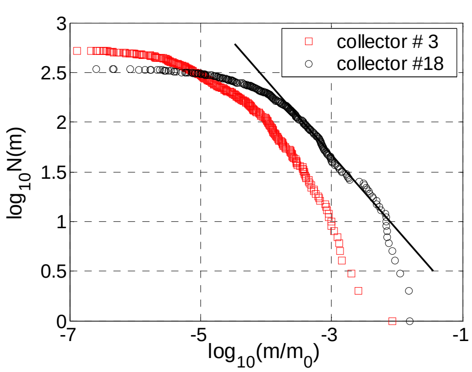

Fig. 13. The cumulative mass distribution for particles recovered from collectors C03 and C18 ($m_0 = 1g$).

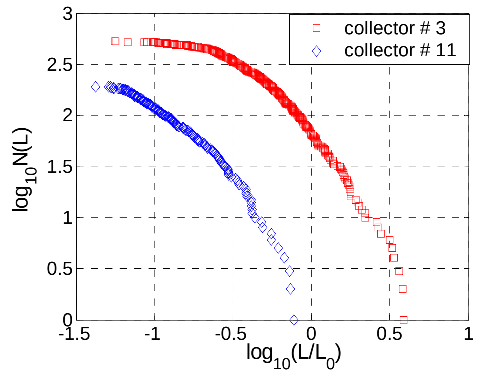

Fig. 14. The cumulative size distribution for particles recovered from collectors C03 and C11 (L_0=1mm)

A more accurate representation of the ejecta masses in the experiments with the 1.45 mm and 3 mm-thick aluminum plates is given by the cumulative mass distributions (Fig.13). In Fig.13 $N(m)$ is the total amount of the ejecta particles whose mass is equal to or larger than m. It is obvious that the experiment with thinner plate gives the greater number of the ejecta particles in a range of small masses. The cumulative size distribution for the ejecta particles in the experiments with the steel mesh and the 1.45 mm-thick aluminum plate of equal areal density is presented in Fig.14. One can see that in all range of sizes the number of the ejecta particles is less in the experiment with the mesh.

As a rule (e.g. [6, 7]) the mass distribution of fragments from high-velocity impacts is a power law for the intermediate masses

$$N(m) \propto m^{-\beta} \tag{1}$$

where $\beta > 0$. In general, the distributions presented in Fig. 13 hardly reveal the power law. Probably this is due to the fact that the distributions in Fig. 13 have cutoff at large masses due to the finite size of the projectile and plate, and that at small masses due to poor recovering of the smallest particles. Nevertheless, we attempted to estimate the value of exponent β for the data of collector C18. The slope of straight line in Fig. 13 gave β = 0.76. This result does not conflict with known experimental data on the fragment mass distributions in impact fragmentation.

3.2 Results of experiments with foils as collectors

The results of the fourteen successful experiments with foils as collectors are presented in Tab. 5. The results of the experiments with the fiber-glass plastic plates shown in Tab.5 (shots F01-F11) can be summed up as following:

- total amount of the glass or plastic-resin ejecta particles is quite large (~400-600) (except experiment with 1mm-thick fiber-glass plate, shot F11 in Tab. 5);
- the maximum angular spread of the particle trajectories measured from the shot line lies approximately within the range of 20^0 to 55^0 ;
- in the spread zone the particles are distributed quite chaotic and the most of them have quite small size;
- perforating ability of the ejecta particles is not high: 80-90% of the particles are not able to perforate the first 0.06 mm-thick aluminum foil; and barely 2-3% of all particles perforate the second foil doing it at ballistic limit (mentioned as B.L. in Tab. 5).

Obviously, there is a sufficient discrepancy between the experimental results for the aluminum plates (shots F12-F14) and those for the fiber-glass plastic plates (shots F1-F11) presented in Tab. 5. One can see that the perforating ability of the ejecta particles is significantly higher in experiments with the aluminum plates: about half of the ejecta particles in these experiments perforate the first foil whose thickness is more than three times greater than the foil thickness in the experiments with the fiber-glass plastic plates.

To estimate the masses of the ejecta particles, which perforate the aluminum foil at ballistic limit condition, a well-known Fish-Summers equation for marginal perforation [8] can be used:

$$t = K_1 \rho_p^{0.52} d_p^{1.056} V_i^{0.875} \tag{2}$$

where t is the target (foil) thickness (cm), K_1 is a constant for the target, d_p is the particle diameter (cm), ρ_p is the particle density (gm/cm^3), V_i is the impact velocity (km/s) and $K_1 = 0.43$ for aluminum alloys.

Taking into account the higher perforating ability of glass particles in comparison with hardened resin particles, which have two-times lower density, the glass particles should be chosen for the use in Eq. 2. Thus, for the estimations with Eq. 2 the following particle densities will be taken: 2.5g/sm^3 for glass particles and 2.7g/sm^3 for aluminum ones.

Numerical modeling of the experiment with 6.35 mm aluminum projectile and 3 mm-thick aluminum plate [9] shows that with the projectile velocity of V_{proj} ~3 km/s the velocity of the fastest ejecta particles, which are situated in the upper part of the ejecta cone, is ~70 % of the projectile velocity. The maximum and minimum velocities of the ejecta particles will be evaluated as $V_{\max} = 0.7 V_{\text{proj}}$ and $V_{\min} = 0.2$ km/s in the experiments F12-F14 with the aluminum plates, and as $V_{\max} = V_{\text{proj}}$ and $V_{\min} = 0.1$ km/s in the experiments F1-F11 with the fiber-glass plastic plates (Tab. 5).

To estimate the sizes of the ejecta particles obtained in the experiments (Tab. 4), we make additional suppositions following the work [1]:

• The amount of the ejection velocity is inversely proportional to diameter of the ejecta particle:

$$V = \frac{D}{d} + E \tag{3}$$

where $D = (V_{\max} - V_{\min}) d_{\min} d_{\max} / (d_{\max} - d_{\min})$ and $E = (V_{\min} d_{\max} - V_{\max} d_{\min}) / (d_{\max} - d_{\min})$, $d_{\min}$ and $d_{\max}$ are the diameters of the smallest particle and the largest one. We consider the case of $E > 0$, which means that the minimum velocity is applied to the largest ejecta particle. The velocities in Eqs. 2 and 3 are connected by the relation $V_i = V \cos\varphi$ where average value of the ejecta cone angle φ is taken from the experiment (Tab.5).

• The differential size distribution of ejecta particles is a power law function:

$$n(d) = N_\Sigma \frac{-\alpha + 1}{d_{\max}^{-\alpha+1} - d_{\min}^{-\alpha+1}} d^{-\alpha}, \ d \in [d_{\min}, d_{\max}], \tag{4}$$

where N_Σ is the total number of ejecta particles. The coefficient $\alpha = 3.5$ is taken for a brittle target and $\alpha =$ 2.6 for a ductile one.

Eqs. (2) and (3) imply the following relation

$$\left(\frac{t}{K_1 \rho_p^{0.52} (\cos\varphi)^{0.875}} \right) = d^{1.056} \left[\left(\frac{D}{d} + E \right) \right]^{0.875} \tag{5}$$

The right side of Eq. 5 is a monotonically increasing function of the particle diameter. Consequently, Eq. 5 for a given foil thickness t has a unique solution for the smallest ejecta particle of a diameter d perforating this foil. The solution of Eq. 5 for a maximum diameter $d_{\max}$ corresponds to the marginal perforation of the two foils (in this case $t = 0.04$ cm or 0.012 cm depending on the experiment). The solution of Eq. 5 corresponding to the marginal perforation of one foil (in this case $t = 0.02$ cm or 0.006 cm), we denote by d_1.

The average mass m_{avr} and diameter d_{avr} of the ejecta particles, and the number of ejecta particles, N_1, perforating the first foil, are estimated by mean of distribution (4):

$$N_1 = \int_{d_1}^{d_{\max}} n(\delta) d\delta = N_\Sigma \frac{1 - (d_1 / d_{\max})^{-\alpha+1}}{1 - (d_{\min} / d_{\max})^{-\alpha+1}}, \tag{6}$$

$$m_{avr} = \frac{1}{N_\Sigma} \int_{d_{\min}}^{d_{\max}} \frac{1}{6} \pi \rho_p \delta^3 n(\delta) d\delta = \frac{1}{6} \pi \rho_p \frac{\alpha - 1}{4 - \alpha} d_{\min}^{\alpha-1} d_{\max}^{4-\alpha}, \tag{7}$$

$$d_{avr} = \sqrt[3]{\frac{6 m_{avr}}{\pi \rho_p}},$$

In deriving Eq. 7 we took into account that $d_{min} << d_{max}$. It should be noted that the values of N_1 и N_Σ in Eqs. 4 and 6 are known from the experiment (Tab. 5).

Eqs. 3-7 and the assumptions made allowed us to obtain a closed system of equations determining d_{min}, d_{max}, d_1 and d_{avr}, and evaluate their values in the experiments presented in Tab.5. Results of these evaluations are presented in Table 6 for shots F02-F04, F09, F12 and F14 in which the marginal perforations occurred. We did not take shot F13 for the evaluation because of the relatively low velocity of projectile in this experiment compared with shots F12 and F14. The results presented in Tab.6 can be summed up as follows:

- First of all, we notice that the accepted value of the minimum velocity V_{min} = 0.2 km/s applied to the largest ejecta particle by Eq. (3) gives a satisfactory fit between the evaluations of the maximum diameter (shots F12 and F14 in Tab.6) and the maximum sizes of the recovered particles (collectors C03 and C18 in Tab. 4) in the experiments with aluminum plates.
- In the experiments with 3 mm-thick aluminum plate the evaluation of the average mass and diameter of the ejecta particles in shot F14 (Tab. 6) gives a good fit with the average mass and size of the recovered particles (collectors C18 in Tab. 4).
- The average mass of the ejecta particles in the experiments with aluminium plates is two orders of magnitude higher than that in the experiments with fiber-glass plastic plates.
- The average diameter of the ejecta particles in the experiments with aluminium plates is about six times more than that in the experiments with fiber-glass plastic plates, while the maximum diameter is only about two times more. This can be explained by the fact that the spectrum of the ejecta particles in the experiments with fiber-glass plastic plates involves a large number of small particles.
- Significant difference in the sizes of the ejecta particles explains why the perforating ability of the ejecta particles in the experiments with the aluminum plates is considerably higher than that in the experiments with the fiber-glass plastic plates.

The foregoing comparisons of the experiments F12-F14 (Tab. 5) with the experiments in which were used low-density foam collectors (Tab.1) can be supplemented by the following. The angles of the ejecta cone in the experiments F12-F14 (Tab. 5) is close to those retrieved from foam collectors (Tab. 3). But the total amount of the ejecta particles fixed by the foils in the experiments F12-F14 (Tab. 5) is less than the total amount of ejecta particles recovered from the foam collectors. It can be explained in the following way. In the experiments with the foils, the side walls were absent unlike experiments with the foam collectors. As can be seen from Fig. 7 and 8 an appreciable number of the ejecta particles falls just on the side walls.

4 CONCLUSIONS

In the present work, the series of impact experiments were performed to study the properties of ejecta generated at high-velocity perforation of thin bumpers made from different constructional materials. The bumpers were: the 1.45 mm and 3.0 mm-thick aluminum alloy plates, the 2 mm-thick fiber-glass plastic plates and meshes weaved of steel wire. The projectiles were the 6.35 mm aluminum spheres (and the 3.2 mm diameter aluminum spheres only for several shots into fiber-glass plastic bumpers). The impact velocities ranged from 1.95 to 3.52 km/s. In the experiments the ejecta particles were captured with low-density foam collectors or registered with the use of aluminum foils. In addition to the study of the ejecta properties we attempted to obtain a comparative evaluation of the ejecta flows generated by these different bumpers. Analysis and processing of the experimental results allowed us to draw up the following conclusions:

1. In the experiments with the aluminum plates, the matter in the ejecta is distributed quite inhomogeneously concentrating in individual jets, which form a cone. The jets form deep channels having different depths in foam collectors. Cumulative distribution of the channel depths corresponds approximately to the power law. In the experiments with the steel meshes and the fiber-glass plastic plates, the jets were not observed in the ejecta cone.
2. Presence of the channels inside of the foam collectors in the experiments with the aluminum plates allowed us to determine the jet trajectories with high accuracy and to measure their slope angles. It turned out that these angles have appreciable dispersion. Moreover, their value (measured from the shot line) decreases as the plate thickness increases.
3. Total mass of the ejecta is significantly greater in the experiments with the aluminum plates than in the experiments with the steel meshes of equal areal density.
4. In the experiments with the fiber-glass plastic plates, the quantitative parameters of ejecta can be assessed with acceptable accuracy using collectors made of closely spaced aluminum foils. This method includes assessment of perforating ability of the ejecta particles.
5. The results of the experiments with the fiber-glass plastic plates revealed that the total amount of ejecta particles in each experiment is quite large and their perforating ability is low: ~80-90% of the ejecta particles are not able to perforate the first foil with 0.06 mm thickness.
6. The spread of the ejecta cone angle is larger in the experiments with the fiber-glass plastic plates than in

the experiments with the aluminum plates. For the fiber-glass plastic targets the ejecta cone angle is approximately within the range of ~20^0 to 55^0 (measured from the shot line).

7. The perforating ability of ejecta particles is significantly higher in the experiments with the aluminum plates than in the experiments with the fiber-glass plastic plates. The estimates show (Tab.6) that this experimental fact can be explained by the significant difference in the masses and sizes of the ejecta particles produced in the experiments with these bumpers.

The results obtained can be applied to the problem of reducing the near-Earth space pollution caused by the ejecta. One can see that they argue against the use of the aluminum plates as first (outer) bumper in spacecraft shield protection. Apparently, the better choice would be the bumpers consisting of 2-3 meshes (not only steel, as well). Ballistic tests carried out in [10] showed that the stacked meshes can be high-quality alternative to the aluminum plate of the same areal density.

5 ACKNOWLEDGEMENTS

This research was supported by the Russian Foundation for Basic Research (project 12-01-00027), the Program of Presidium of Russian Academy of Science (program No.25).

6 REFERENCES

1. Rival, M. & Mandeville, J.C. (1999). Modeling of ejecta produced upon hypervelocity impacts. *Space Debris*, **1**, 45–57.
2. Bariteau, M. & Mandeville, J.-C. (2002). Modelling of ejecta as a space debris source. *Space debris*, **2**, 97–107.
3. Christiansen, E.L. & Kerr, J.H. (1993). Mesh double-bumper shield: a low-weight alternative for spacecraft meteoroid and orbital debris protection. *Int. J. Impact Engng.* **14**, 169-180.
4. Bezrukov, L.N., Gadasin, I.M., Kiselev, A.I. et al. (2000). About the Physical Bases of Building the Protection of the ISS Module "Zarya" against Impact Damage by Near-Earth Space Debris Fragments. *Cosmonautics and Rocket Engineering*. **18**, 140-151.
5. Schonberg, W.P. (2001). Characterizing secondary debris impact ejecta. *Int. J. Impact Engng.* **26**, 713-724.
6. Myagkov, N.N. & Shumikhin T.A. (2005). Critical behavior and energy dependence of mass distributions in impact fragmentation. Physica A, **358**, 423-436.
7. Hartmann, W.K. (1969). Terrestrial, lunar, and interplanetary rock fragmentation. *Icarus* **10**, 201-213.
8. Berthoud, L. & Mandeville, J.C. (1993). Empirical Impact Equations and Marginal perforation. In *Proceedings of the First European Conference on Space Debris*, Darmstadt, Germany, 5-7 April 1993, (ESA SD-01), pp. 459-464.
9. Myagkov, N.N.& Shumikhin,T.A.(2010). Modeling of Ejecta Arising from the Spherical Projectile Impact against a Solid Plate**.** *Mehanika Kompozicionnyh Materialov i Konstrukcij*. **16**, 470-483 (in Russian).
10. Bezrukov. L., Myagkov. N., Shumikhin, T. (2009). Ballistic Properties of Mesh Shield Protection at Hypervelocity Impact. In 5*th European Conference on Space Debris,* (ESA, Darmstadt, Germany, March 30-April 2, 2009). *Book of Abstracts*, p. 85.

Table 1. Experimental shots and recovered mass of ejecta

Collector (Shot) #	Velocity (km/s)	Target: thickness(mm) / areal density (kg/m^2)	Recovered mass (g)
C01	2.23	Aluminum (AMg6) plate: 1.45 / 3.88	0,0656
C02	2.65	Aluminum (AMg6) plate: 1.45 / 3.88	0,0781
C03	2.66	Aluminum (AMg6) plate: 1.45 / 3.88	0,0549
C04	2.64	3 steel meshes: 1.0mm × 0.32mm / 2.82	0,0187
C05	2.52	3 steel meshes: 1.0mm × 0.32mm / 2.82	0,0154
C06	3.19	3 steel meshes 1.0mm × 0.32mm / 2.82	0,0166
C07	2.70	Aluminum (AMg6) plate: 3.0 / 8.10	-
C08	2.83	Aluminum (AMg6) plate: 3.0 / 8.10	-
C10	2.91	Steel mesh: 2.0 mm × 1.0 mm /3.83	0,045
C11	2.61	Steel mesh: 2.0 mm × 1.0 mm / 3.83	0,019
C12	2.40	Steel mesh: 2.0 mm × 1.0 mm / 3.83	0,103
C14	2.62	Aluminum (AMg6) plate: 3.0 / 8.10	0,033
C18	2.47	Aluminum (AMg6) plate: 3.0 / 8.10	0,244

Note:
In all shots (C01-C18) the projectiles were 6.35 mm diameter aluminum spheres.

Table 2. Individual ejecta jet angles for collector C07.

Channel I	Channel II	d_c (мм)	φ_{I}	φ_{II}	$(\varphi_{\mathrm{I}}+\varphi_{\mathrm{II}})/2$
The group of the minor diameters					
17	18	86	35	35.5	35.25
2	7	83	34	38	36
14	15	89.5	39	35	37
19	20	87	42	37	39.5
The group of the major diameters				Average:	~ 37
12	16	101	39	43.5	41.25
5	10	97	42	43	42.5
6	11	100	43	43	43
				Average:	~ 42

Table 3. Ejecta cone angles for collectors C01 and C07

Shot/Collector	Velocity (km/s)	Target, thickness	Angles of the ejecta cone (φ)
C01	2.23	Aluminum (AMg6) plate, 1.45 mm	45-48
C07	2.70	Aluminum (AMg6) plate, 3.00 mm	37-42

Table 4. Data for the recovered particles

Collector #	Target: thickness, areal density	Total number of recovered particles	Mass of the greatest particle, g.	Average mass of the particles, g.	Maximum sizes, L/W, mm	Average sizes, L/W, mm
C03	Aluminum plate, 1.45mm, 3.88kg/m2	527	8.5613e-003	1.04e-04	3.86 / 2.68	0.58 / 0.38
C011	Steel mesh (2mm x 1mm), 3.83 kg/m2	191	1.7580e-003	-	0.77 / 0.45	0.175 / 0.132
C018	Aluminum plate, 3.0 mm, 8.10 kg/m2	343	1.5562e-002	7.11e-04	4.5 / 2.32	0.99 / 0.65

Table 5. Experiments with metallic foil witnesses

Shot #	Material and thickness of targets, (mm)	Diameter of a spherical aluminum projectile, (mm)	Projectile velocity, km/s	Total amounts of particles (roughly)	Angle of spreading (from shot line) (degree)	Amounts of particles that perforate the first foil	Amounts of particles that perforate the second foil
F01	KAST-V, 2	6.35	2.15	400	20-43	40	0
F02	KAST-V, 2	6.35	2.84	400	20-40	53	3(~B.L.)
F03	KAST-V, 2	6.35	3.30	450	18-45	80	9 (~B.L.)
F04	KAST-V, 2	6.35	3.52	500	17-50	80	5 (~B.L.)
F05	KAST-V, 2	3.2	3.44	500	18-55	20	0
F06	KAST-V, 2	3.2	3.10	500	18-44	23	0
F07	VFT-S, 2	6.35	2.38	500	17-47	75	12(~B.L.)
F08	VFT-S, 2	6.35	3.13	650	20-52	110	0
F09	VFT-S, 2	6.35	3.01	600	18-50	70	4(~B.L.)
F10	VFT-S, 2	3.2	2.47	400	20-42	45	0
F11	VFT-S, 1	3.2	2.74	150	20-40	2(B.L.)	0
F12	AMg6, 1.5	6.35	3.19	250	38-51	80	3(~B.L.)
F13	AMg6, 3	6.35	1.95	120	37-48	70	4(~B.L.)
F14	AMg6, 3	6.35	2.97	300	34-55	150	15(~B.L.)

Notes:

1. In experiments (##01-11) three spaced 0.06 mm-thick aluminum foils were used as collectors.
2. In experiments (##12-14) three spaced aluminum foils of different thickness were used as witnesses (two of them, the frontal ones, were 0.2 mm-thick aluminum foils and the third was 0.06 mm-thick aluminum foils).
3. B.L. means ballistic limit.

Table 6

Shot from tab. 6 #	Minimum diameter $d_{\min}$, mm	Maximum diameter $d_{\max}$, mm	d_1, mm	Average mass m_{avr}, g	Average diameter d_{avr}, mm
F02	$4.68\cdot10^{-2}$	1.63	0.105	$3.97\cdot10^{-6}$	0.145
F03	$4.27\cdot10^{-2}$	1.65	$8.54\cdot10^{-2}$	$3.18\cdot10^{-6}$	0.135
F04	$4.10\cdot10^{-2}$	1.68	$8.52\cdot10^{-2}$	$2.88\cdot10^{-6}$	0.130
F09	$4.58\cdot10^{-2}$	1.69	0. 108	$3.82\cdot10^{-6}$	0.143
F12	0.210	3.25	0.417	$6.92\cdot10^{-4}$	0.788
F14	0.237	3.25	0.360	$8.40\cdot10^{-4}$	0.841